

Design Parameters for DIII-D Steady-State Scenario Discharges

J.R. Ferron¹, C.T. Holcomb², T.C. Luce¹, J.M. Park³, P.A. Politzer¹, F. Turco⁴, J.C. DeBoo¹,
E.J. Doyle⁵, A.W. Hyatt¹, Y. In⁶, R.J. La Haye¹, M. Murakami³,
M. Okabayashi⁷, T.W. Petrie¹, C.C. Petty¹, H. Reimerdes⁸, T.L. Rhodes⁵, A.E. White⁹,
and L. Zeng⁵

¹General Atomics, PO Box 85608, San Diego, California 92186-5608, USA

²Lawrence Livermore National Laboratory, Livermore, California 94550, USA

³Oak Ridge National Laboratory, Oak Ridge, Tennessee 37831, USA

⁴Oak Ridge Associated Universities, Oak Ridge, Tennessee 37831, USA

⁵University of California-Los Angeles, Los Angeles, California 90095, USA

⁶FAR-TECH, Inc., 3550 General Atomics Ct, San Diego, California 92121, USA

⁷Princeton Plasma Physics Laboratory, PO Box 451, Princeton, New Jersey 08543 USA

⁸CRPP-EPFL, CH-1015 Lausanne, Switzerland

⁹Massachusetts Institute of Technology, Cambridge, Massachusetts, USA

In recent DIII-D experiments [1-3], we have systematically studied the physics that affects the choice of parameters for a discharge where the goal is 100% noninductively driven current ($f_{NI}=1$) at high plasma pressure ($\beta_N \geq 4$). The choice of parameters will be a compromise that results in sufficiently high values of the bootstrap current fraction f_{BS} , the efficiency of the externally driven current, and the fusion gain parameter $G = \beta_N H/q_{95}^2$ [4]. The available adjustable parameters are the q profile, the toroidal field B_T , and the plasma density n . The tokamak geometry and the discharge shape are constrained by the existing DIII-D design. β_N will be close to the stability limit, which must be high enough to give access to the required f_{BS} and G . The input power is that required for external current drive at $f_{NI}=1$ and it must match the power required to maintain the pressure against transport losses [4].

To assess the effect of the q profile [2], the self consistent response of the temperature (T) and density profiles was measured in two sets of discharges with q_{min} and q_{95} varied independently (q_{95} is the value of q near the discharge boundary and q_{min} is the minimum value), one set at $\beta_N \approx 2.8$ and one set with the maximum available neutral beam power injected ($\beta_N \approx 3.5$ in most cases). The focus was on weak shear discharges without large, local pressure gradients that would reduce the stable β_N . The effects on stability and transport of more detailed features of the q profile such as the profile of the magnetic shear and the radial location where $q=q_{min}$, also important for the choice of steady-state scenario parameters, will be considered in future work. Changes in the measured n and T profiles resulted in a systematic broadening of the pressure profile as either q_{min} or β_N was increased. At the maximum β_N , the peaking factor for the thermal pressure f_p is roughly independent of q_{min} and q_{95} .

The calculated f_{BS} for the experimental data is maximum at the largest value of q_{95} and the largest values of β_N (Fig. 1), with variation of f_{BS} with q_{core} comparable to the variation with q_{95} . At $\beta_N \approx 2.8$, the trend is for f_{BS} to increase with q_{core} except at $q_{core} \approx 2$ where the relatively high q_{core} is offset by reduced T and n gradients. At the maximum beam power, f_{BS} increases

with q_{core} at the lowest q_{95} values, but at $q_{95}=6.8$ the scaling is the opposite because at the lowest q_{core} , β_N was relatively high (3.8) and at the highest q_{core} , β_N was relatively low (3.1). The neutral beam current drive fraction [2] was highest in the relatively low n discharges at the highest q_{core} , so that the calculated f_{NI} , in most cases, also increases with both q_{core} and q_{95} (Fig. 2).

At the highest values of β_N the reduced f_p results in J_{BS} profiles which are relatively uniform in the region inside the H-mode pedestal (Fig. 3). This J_{BS} profile shape is not a good match to the peaked profile of current density J in weak shear discharges. In addition, J_{BS} is only a small fraction of J in the inner portion of the discharge. Therefore, to achieve $f_{\text{NI}}=1$, the profile of the externally driven noninductive current that results in a match between the total noninductive current density J_{NI} and J will need to be peaked on axis.

The scan of the q profile indicates that $f_{\text{NI}}=1$ with $f_{\text{BS}}>0.5$ is presently best achieved in DIII-D at $q_{95}>6$. The preferable q_{min} value is relatively high (e.g. >2) to minimize the external current drive requirement near the axis by reducing J and increasing J_{BS} in that region, but β_N must be increased above the value observed at the highest q_{core} value in this experiment. An excess of externally-driven current density near the axis which reduces q_{min} , as in the case in Fig. 3, must be avoided. This is possible through injection of a substantial fraction of the neutral beam power off-axis, consistent with the case in Fig. 3 where $\approx 20 \text{ A cm}^{-2}$ additional J_{NI} is required in the region $0.2 < \rho < 0.7$ at $q_{95}>6$ in order to reach $f_{\text{NI}}=1$. The capability to inject 5 MW off-axis has been made available for 2011 DIII-D experiments. Modeling of a discharge with 5 MW on-axis beam injection, 5 MW off-axis injection, and 3.5 MW off-axis ECCD predicts $q_{\text{min}}=2$ with a fully penetrated electric field.

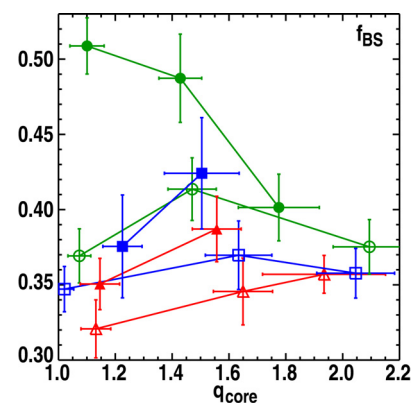


Fig. 1. Calculated bootstrap current fraction. $\beta_N=2.8$ (open), maximum beam power (closed), q_{95} : 4.5 (triangles), 5.6 (squares), 6.8 (circles). q_{core} is the average value of q in the region $0.0 < \text{normalized radius } \rho < 0.3$.

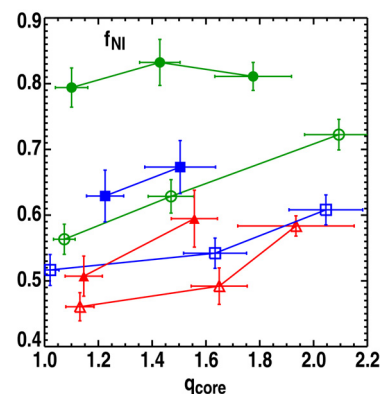


Fig. 2. Noninductive current fraction. Symbols are as in Fig. 1.

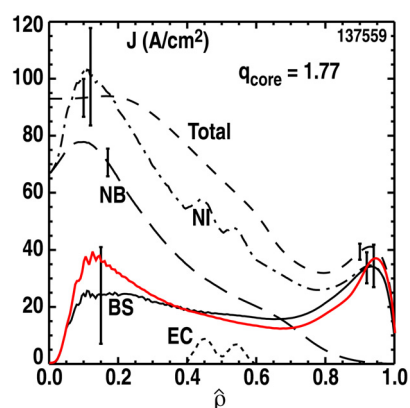


Fig. 3. Current density profiles in a discharge with the maximum neutral beam power, $q_{95}=6.8$, $q_{\text{core}}=1.77$. The total is from an equilibrium reconstruction, bootstrap (BS), electron-cyclotron (EC), neutral beam (NB) and total noninductive (NI) are calculated. The red curve is bootstrap at $\beta_N \approx 2.8$.

In order to satisfy the requirements on the figure of merit G in the steady-state scenario of ITER or in a reactor, $q_{95} \approx 5$ is thought to be necessary. The small value of $f_{BS} \approx 0.4$ observed in this experiment at $q_{95} \approx 5$, though, is not sufficient for practical steady-state operation. As q_{95} is reduced with fixed q_{min} , the additional current density is located off axis. The primary path to increased f_{BS} with J_{BS} added off-axis is broadening of the pressure profile to allow stable operation at increased β_N . Broadening of the pressure profile increases n and T gradients off-axis, and thus J_{BS} there, and results in higher stability limits. For MHD stability, the peaking factor for the fast ion pressure must be comparable to f_p so that the total pressure peaking factor is low. This will be facilitated by off-axis neutral beam injection in DIII-D. Previous estimates have found ideal-wall stability at $\beta_N = 4$ with total pressure peaking factor less than 2.6 [5].

At fixed β_N and q_{95} , the toroidal field strength (B_T) is the parameter to adjust to obtain a balance between the required current drive (P_{CD}) and heating powers when all external power sources provide both heating and current drive [3]. In cases like DIII-D where there is no α -heating, the fraction of I_p driven by external current sources f_{CD} would be expected to increase with B_T as a result of the scaling of energy confinement with input power. Assuming H_{89p} confinement scaling, $P_{CD} \propto B_T^{1.9}$ at constant β_N and q_{95} , and for current drive efficiency of the form [4] $nI_{CD}/(P_{CD}T_e)$, then $f_{CD} = C_{CD} P_{CD} \beta_N q_{95}^2 / (B_T f_G^2) \propto B_T^{0.9}$ (where f_G is the Greenwald density fraction and C_{CD} is a constant). If n is maintained at a low level through pumping of divertor exhaust so that f_G decreases as B_T is increased, the driven current increases faster than linearly with P_{CD} because of increases in T_e . This type of scaling was demonstrated in DIII-D in a series of neutral-beam-heated discharges [3] with $q_{95} = 6.2$ and $\beta_N \approx 3.4$ (Fig. 4). A factor 1.2 change in B_T required a factor 1.4 increase in the neutral beam power, resulting in a factor 1.6-1.8 increase in the total neutral beam driven current. Because B_T/I_p was held constant during the scan, f_{NBCD} and f_{NI} also increased.

In DIII-D steady-state scenario experiments, the minimum achievable n is used in order to maximize f_{CD} . To minimize n , the plasma shape is chosen to optimize the use of the divertor cryopump capability [1]. Typically $H_{98} = 1.5$ as long as n is above approximately $4.5 \times 10^{19} \text{ m}^{-3}$, but as n decreases during the high β_N phase of a discharge as the wall particle source is depleted, a trend toward decreasing τ_E is observed (Fig. 5). This places constraints on the ability to reduce n in order to maximize the total externally driven current. No reproducible

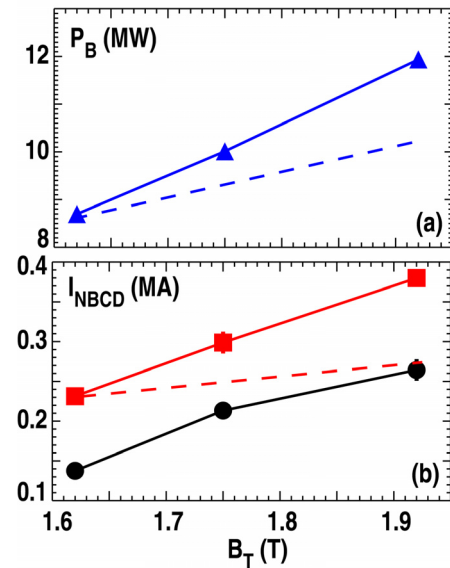


Fig. 4. As a function of the toroidal field strength (a) neutral beam power at constant β_N , (b) total neutral-beam-driven current. The dashed lines show the trend that would be expected from scaling which is linear in B_T . Anomalous fast ion diffusion: none (red), 1-2 m^2/s (black).

quantitative relation between n and H_{98} has been found as yet, but for n near $4.0 \times 10^{19} \text{ m}^{-3}$, H_{98} typically is about 1.1.

A set of self-consistent parameters for $f_{\text{NI}}=1$ operation in DIII-D can be determined by combining the observed scalings of f_{BS} and f_{CD} . A fit to the data from the q profile scaling experiment yields $C_{\text{CD}} = 1.03 \times 10^{-4}$ and f_{BS} scales with β_{N} , q_{core} , q_{95} and f_{p} as shown in [2]. In the example in Fig. 6, the circles highlight $f_{\text{NI}}=1$ solutions at two values of q_{95} . At $q_{95} \approx 6.2$, $f_{\text{NI}}=1$ at $\beta_{\text{N}}=3.8$ (similar to the discharge discussed in [1]). For the heating and current drive powers to be balanced, the required confinement enhancement factor H_{89} , 2.1 in this case, must match the value in the discharge. At $q_{95} \approx 5$, the $f_{\text{NI}}=1$ solution is at higher $\beta_{\text{N}}=4.1$, requiring a larger $H_{89}=2.3$. To adjust the power balance, B_{T} can be changed. For instance, for the parameters of Fig. 6 but at higher $B_{\text{T}} = 2.0 \text{ T}$, the $f_{\text{NI}}=1$ solution at $q_{95} \approx 6.2$ is at lower $\beta_{\text{N}}=3.6$ but higher $H_{89}=2.2$, and at $q_{95} \approx 5$ the solution moves to $\beta_{\text{N}}=3.85$, $H_{89}=2.5$. In all cases, MHD stability must be sufficient to reach the required β_{N} .

Work supported in part by the US Department of Energy under DE-FC02-04ER554698, DE-AC52-07NA27344, DE-AC05-06OR23100, DE-FG02-08ER54984, DE-FG02-06ER84442, DE-AC05-00OR22725, DE-AC02-09CH11466 and DE-FC02-99ER54512.

[1] C.T. Holcomb *et al.*, 2009 Phys. Plasmas **16** 056116

[2] J.R. Ferron *et al.*, 2011 Nucl. Fusion **51** 063026

[3] J.R. Ferron *et al.*, 2011 “Balancing Current Drive and Heating in DIII-D High Noninductive Current Fraction Discharges,” submitted to Nucl. Fusion (2011).

[4] C. Gormezano *et al.*, 2007 Nucl. Fusion **47** S285

[5] J.R. Ferron *et al.*, 2005 Phys. Plasmas **12** 056126

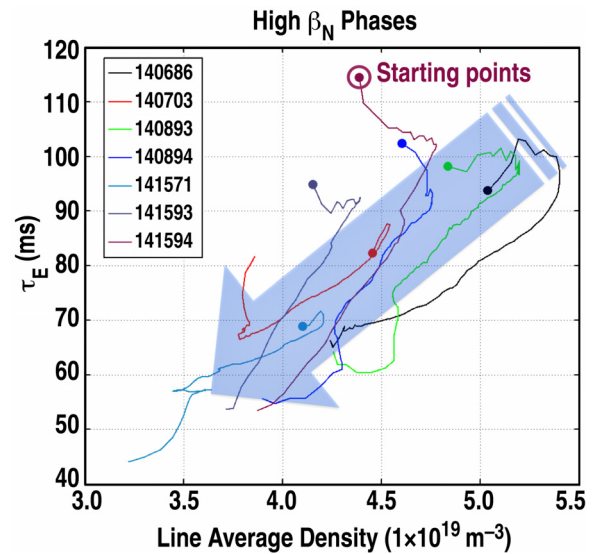


Fig. 5. For several discharges, in the approximately constant $\beta_{\text{N}} > 3$ phase, energy confinement time as a function of density.

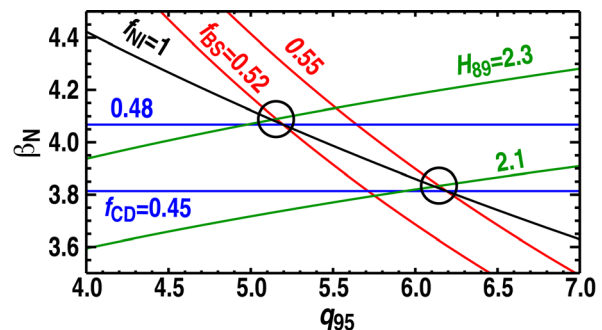


Fig. 6. Contours of self-consistent discharge parameters derived from f_{BS} and f_{CD} scalings and $f_{\text{NI}}=f_{\text{BS}}+f_{\text{CD}}$ with $B_{\text{T}}=1.75 \text{ T}$, $q_{\text{core}}=2$, $n=4.5 \times 10^{19} \text{ m}^{-3}$, $f_{\text{p}}=2.5$, $P_{\text{CD}}=16 \text{ MW}$, and fast ion stored energy fraction = 0.25. The circles highlight $f_{\text{NI}}=1$ solutions at two values of q_{95} .